Appl. Phys. A (2016) 122:352
DOI 10.1007/s00339-016-9834-z

Applied Physics A
Materials Science & Processing

The influence of laser alloying on the structure and mechanical properties of $AlMg_5Si_2Mn$ surface layers

W. Pakieła[1] · T. Tański[1] · Z. Brytan[1] · K. Labisz[1]

Received: 22 September 2015 / Accepted: 17 February 2016 / Published online: 10 March 2016

Abstract The goal of this paper was focused on investigation of microstructure and properties of surface layer produced during laser surface treatment of aluminium alloy by high-power fibre laser. The performed laser treatment involves remelting and feeding of Inconel 625 powder into the aluminium surface. As a base metal was used aluminium alloy $AlMg_5Si_2Mn$. The Inconel powder was injected into the melt pool and delivered by a vacuum feeder at a constant rate of 4.5 g/min. The size of Inconel alloying powder was in the range 60–130 μm. In order to remelt the aluminium alloy surface, the fibre laser of 3 kW laser beam power has been used. The linear laser scan rate of the beam was set 0.5 m/min. Based on performed investigations, it was possible to obtain the layer consisting of heat-affected zone, transition zone and remelted zone, without cracks and defects having much higher hardness value compared to the non-alloyed material.

✉ T. Tański
tomasz.tanski@polsl.pl

W. Pakieła
wojciech.pakiela@polsl.pl

Z. Brytan
zbigniew.brytan@polsl.pl

K. Labisz
krzysztof.labisz@polsl.pl

[1] Division of Materials Processing Technology, Management and Computer Techniques in Materials Science, Institute of Engineering Materials and Biomaterials, Silesian University of Technology, Konarskiego Str 18A, 44-100 Gliwice, Poland

1 Introduction

Growing demands on the mechanical properties and weight reduction of components in automotive and aerospace industries cause that more and more frequently in a such kind of applications the light alloys such as aluminium and magnesium are used [1, 2]. The disadvantage of this group of metals is relatively low mechanical properties and hardness [2–4]. Aluminium also has high thermal and electrical conductivity, good electromagnetic shielding characteristics, good machinability and is easily recycled. Moreover, a great advantage of aluminium is much better corrosion resistance than in the case of magnesium alloys. Relatively poor mechanical and wear properties of aluminium alloys can be improved in many ways [5]. The most common are the used classic heat treatment. There are also reports of the improving of mechanical property in this group of light alloys by the use of PVD coatings [6].

At the turn of the last few years, there has been a growing interest in improving the mechanical and tribological properties of all metal alloys by laser techniques [7–11]. Currently, more frequently to improve surface properties of metallic materials the laser surface treatment is applied such as melting, cladding and surface alloying. The use of a laser surface treatment allows obtaining a layer of high thickness (usually about 1 mm) and good mechanical properties [3, 11, 16–21].

Preliminary studies and review of the literature have shown that intermetallic phases based on aluminium, nickel and chrome having high mechanical properties provide high wear resistance and excellent corrosion resistance and oxidation at high temperature when laser-alloyed [12–15].

The main objective of this study was focused on fibre laser alloying of aluminium alloy $AlMg_5Si_2Mn$ by a Inconel EL-625 alloy powder and evaluation of resulted

Table 1 Chemical composition of investigated aluminium alloy

Elements	Fe	Si	Mn	Ti	Cu	Mg	Zn	Al
$AlMg_5Si_2Mn$	Max 0.25	1.8–2.6	0.4–0.8	Max 0.25	Max 0.05	4.7–6	Max 0.07	Rest

Table 2 Chemical composition of applied powder Inconel EL-625

Elements	Ni	Cr	Fe	Mo	Nb	Co	Mn	Al	Ti	Si
EL-625	58.0	20.0–23.0	5.0	8.0–10.0	3.15–4.15	1.0	0.5	0.4	0.4	0.5

surface microstructure and properties, in particular hardness and abrasion resistance.

2 Experimental procedure

The research was carried out on cast aluminium alloy with magnesium and silicon EN AC-$AlMg_5Si_2Mn$. The chemical composition of applied alloy is shown in Table 1. For the laser alloying, the spherical powder of Inconel EL-625 alloy with chemical composition shown in Table 2 was used. The grain size of the metal powder was in the range from 60 to 130 μm (Fig. 1). The alloying powder was dried before laser alloying in a dryer for 12 h at 150 °C in order to completely eliminate moisture, which, as indicated by preliminary studies, was primarily responsible for harmful porosity found on the alloyed surface. Samples before surface laser alloying were ground mechanically on laboratory LaboPol 5 Struers grinding machine with sandpaper of 15 μm grain size. Next, thus prepared sample surface was covered with a flux consisting of a mixture of lithium chloride and ethyl alcohol and then dried on a hot plate at a temperature of 110 °C. Application of above the flux allowed to dissolve metal oxides formed on the surface of aluminium substrate and significantly increased the adsorption of laser radiation by processed metal.

Aluminium laser surface alloying was performed by means of fibre Ytterbium Laser System YLS-4000 with a wavelength of $\lambda = 1070$ nm, maximum laser beam power of 4000 W, mounted on a 6-axis robot REIS RV30-26 coupled with a tilt-and-swivel positioning system. During the surface treatment has been applied rectangular laser spot size 2 × 6 mm. The laser alloying process was conducted in a shielding gas atmosphere of argon served with two nozzles. The first nozzle was directed at the alloying area at 45° and served as a protection of the melt pool. The second nozzle was pointing the alloying area at 25°, and it was used to feed alloying powder. The parameters of the laser alloying are shown in Table 3.

The microstructure of studied layers was examined by light microscope Axio Observer and a scanning electron microscope Zeiss Supra 35 using secondary electrons and backscattered one (SE, BSE images). The surface topography was observed using a stereomicroscope SteREO Discovery Zeiss. The TEM thin film analysis was carried out in a high-resolution transmission electron microscope S/TEM TITAN 80–300 of FEI company equipped with a STEM scanning system with the following conditions: accelerating voltage of 300 kW, aperture size of 10 μm, camera length of 330 mm and a single-wavelength anomalous diffraction (SAD) technique to collect diffraction data.

Table 3 Parameters of the laser alloying

Laser beam power (kW)	3 kW
Shielding gas (l/min)	
First nozzle	5
Second nozzle	10
Powder feeding (g/min)	4.5
Sample initial temperature (K)	373
Laser beam scanning rate (m/min)	0.5

Table 4 Ball-on-disk wear test parameters

Load (N)	5
Linear speed (cm/s)	15
Distance (m)	150
Radius (mm)	2.5
Counter-specimen	ball—Al_2O_3

The wear resistance studies of surface layers were performed using a rotating sample test the ball-on-disk. Test parameters are shown in Table 4. Additionally, during the ball-on-disk test, the friction coefficient between tested sample and ceramic counter-specimen made of Al2O3 was registered. The wear tracks after the test were measured with a profilometer Surtronic 25 Taylor-Hobson and imaged using a confocal microscope. When measuring the surface roughness by profilometer, the Gaussian filter of 0.25 was applied. The wear track was analysed using a scanning electron microscope in order to reveal rifts and deformation of the surface layer and evaluate wear mechanism. The chemical analysis of processed surface layers was performed using the scattered X-ray detector EDS.

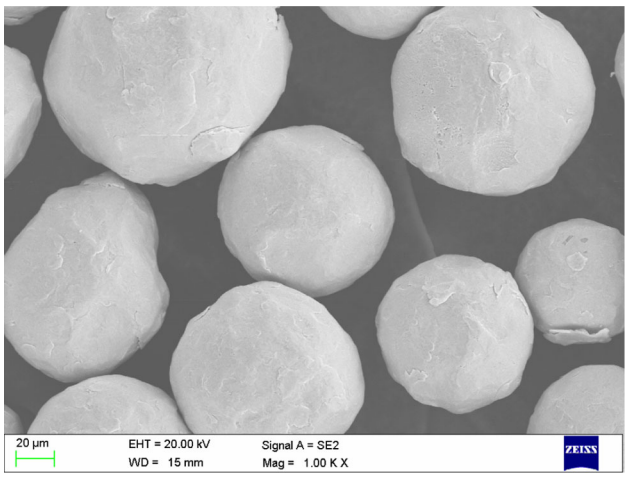

Fig. 1 Morphology of Inconel 625 powder applied to aluminium laser surface alloying

The surface hardness measurements were performed using a Rockwell test in HRA scale, while the microhardness on the layers cross section was measured by the Vickers microhardness test with a force of 300 gf (2.94 N).

3 Results and discussion

Laser surface alloying of $AlMg_5Si_2Mn$ by spheroidal powder particles of Inconel 625 alloy resulted in homogeneous, hard and wear-resistant surface layer. The analysis of metallographic results shows that applied surface treatment allows obtaining a composite surface layer characterized by a relatively flat and smooth face with no visible cracks, voids and porosity of the surface. The waviness profile analysis revealed that the average height difference between the highest and the lowest surface elevation does not exceed 100 µm, and such type of surface geometry is caused by the differences in the laser power density in different sample areas and a rectangular geometry of the laser beam itself. In addition, on the surface layer few undissolved particles used for the alloying powder were identified (Fig. 2a). The average surface roughness of laser-processed layers was included in the range from 0.83 to 2.15 µm. The surface waviness and roughness profiles are shown in Fig. 2b.

The microstructure analysis, on the cross section, of laser-treated surface has not revealed any presence of undissolved alloying powder particles Inconel 625, either visible cracks, discontinuities, or porosity, that may lower the strength properties and their overall performance, thus indicating the proper selection of laser alloying process parameters, such as scanning speed, laser beam power, powder feeding rate and the portion of shielding gas. When analysing alloying depth, it

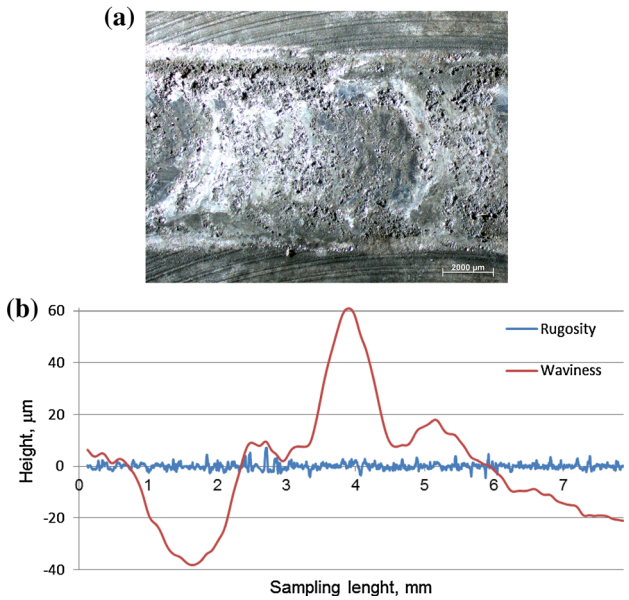

Fig. 2 Composite surface layer obtained on the $AlMg_5Si_2Mn$ alloy by Inconel laser alloying; **a** the surface topography, mag. 15×; **b** the surface waviness and roughness profiles of processed

was shown that the thickness of resulting layer is not constant over the entire length of the alloying. At the beginning of the alloying length (up to 20 mm from the start of melting), the depth of the layer varies in the range of 113–193 µm. This phenomenon is caused by the temperature effect on the thermophysical properties of aluminium alloy and therefore on absorption and heat distribution in the sample. The depth of alloying is stabilizing after 20 mm of the process length. The average depth of the layer is included in the range from 190 to 225 µm. The resulting microstructure in alloyed surface shows an even and uniform layer in the entire cross section and is characterized by uniform distribution of alloying powder in the remelting volume.

Microstructure of alloyed layer is composed of the matrix of solid solution of magnesium in aluminium with visible many acicular precipitations of Al_8Cr_5 phase, between which crystallized spheroidal precipitates rich in aluminium and nickel—Al_3Ni and Al_3Ni_2 phases (Fig. 3b). In the alloying zone can be distinguished two areas formed by the convective movements occurring in the liquid pool during laser alloying. Moreover, due to convection, on the border of alloyed layer and aluminium substrate occurred numerous metal turbulences resulting in uneven shape of the layer bottom (Fig. 3a). The light microscopy studies revealed the presence of three zones in the alloying area. Starting from the top surface, the first zone of alloying layer covers a melted area rich in phases created by alloying. The contact area between melted zone and the substrate material is an intermediate zone, partially melted and enriched in precipitating phases (Figs. 3, 12). During

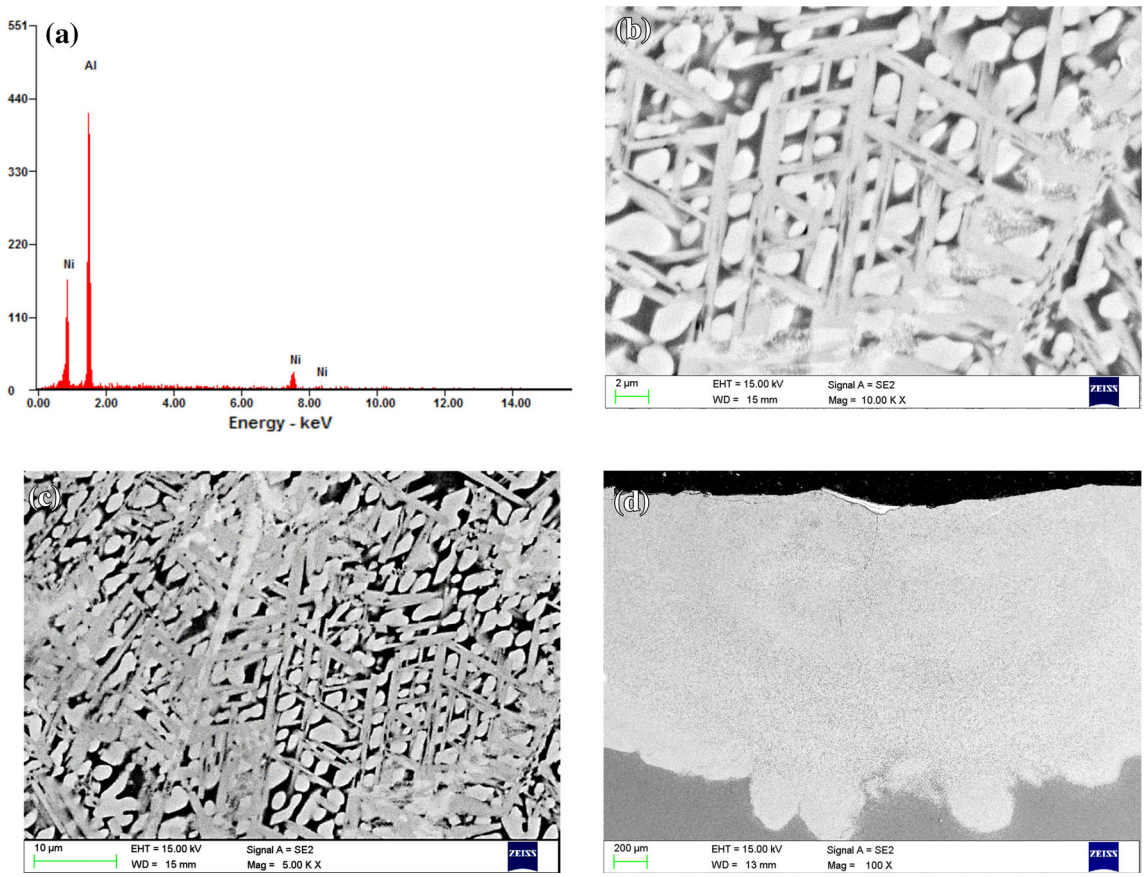

Fig. 3 Laser-alloyed aluminium $AlMg_5Si_3Mn$ with Inconel 625; **a** EDS point analysis, **b**, **c** alloyed area about 150 µm from the weld face and **d** cross section of laser composite surface aluminium

metallographic analysis also, the heat-affected zone (HAZ) was revealed with the thickness not exceeding 150 µm. The microstructure in the top of alloyed surface is shown in Fig. 3.

During EDS analysis, due to the complex chemical composition of the substrate metal and alloying powder applied to laser alloying, a detailed analysis was performed for most frequently occurring phases rich in aluminium, nickel and chromium. Observed phases were identified on the basis of microstructural morphology and chemical composition analysis, the phase equilibrium diagrams and the analysis of thin film in transmission electron microscopy (Figs. 4, 5, 6, 7). During laser surface alloying and occurring in situ reactions, the whole volume of the resulting composite surface layer shows predominance of intermetallic phases rich in aluminium, chromium and nickel (Al_3Ni, Al_3Ni_2, Al_8Cr_5), aluminium and iron $Al_{13}Fe_4$ and a few precipitates composed of aluminium and niobium-Al_3Nb and the ternary phase ρ of chemistry $Al_{75}Cr_{22}Ni_4$ [12, 22–25].

The TEM analysis of the thin films confirmed presence of precipitates composed of nickel and iron with a size not exceeding 10 µm. Furthermore, TEM analysis also revealed phases containing Cr, Mn, Mo, Nb and Mo (Figs. 4, 5).

Wear resistance of base aluminium alloy $AlMg_5Si_2Mn$ and the surface layer obtained by laser alloying with Inconel powder examined during tribological ball-on-disk test confirmed a significant increase in wear resistance of the resulting laser-alloyed composite layer. The wear track of non-alloyed aluminium base alloy shows numerous pull-out areas and plastic deformation of the base metal (Fig. 8a). The pull out areas and plastic deformation of the surface, resulting from adhesion wear of counter specimen in contact with substrate material, contribute to non-uniform abrasive wear of non-alloyed aluminium surface. The effect of non-uniform wear can also be observed when analysing the graph of friction coefficient as a function of test distance. The average roughness of the wear track of non-alloyed aluminium alloy was $R = 1.32$. The wear track of the laser-alloyed composite layer after ball-on-disk test was smooth with little grooves, without cracks and voids. The wear track topography analysis showed uniform and homogeneous nature of the wear (Fig. 8b). The surface roughness of the resulting wear track was 0.21. Analysing wear test results, it was found that the wear depth of the laser-alloyed surface layer, rich in intermetallic phases, was about 4.5 times smaller than the wear of non-alloyed

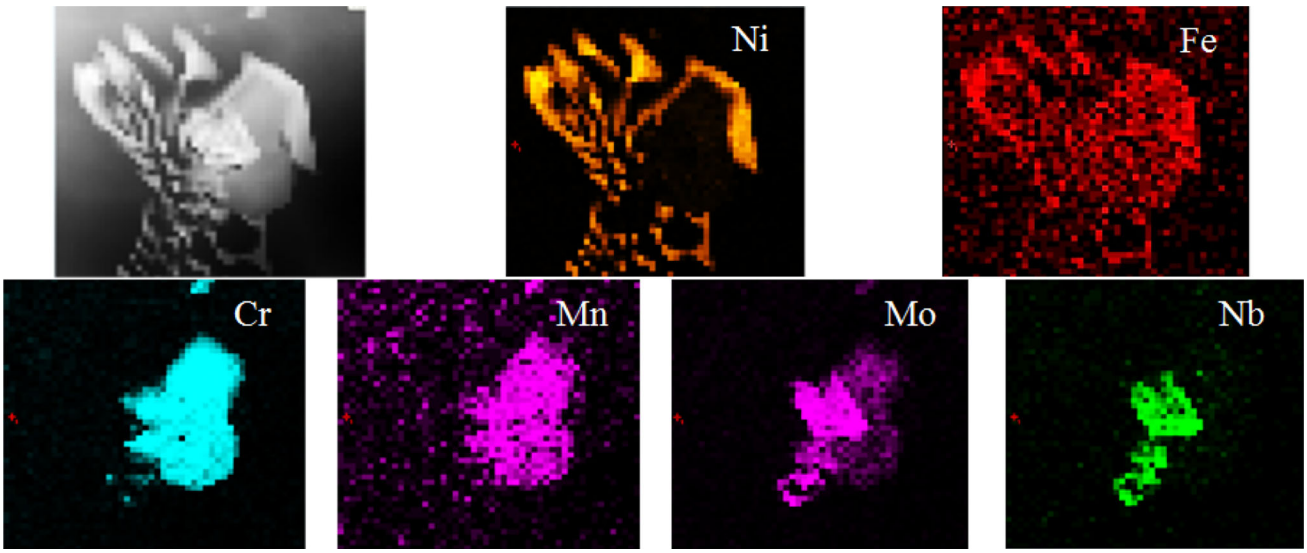

Fig. 4 Maps of the distribution of alloying elements in the analysed area of thin film during TEM observation

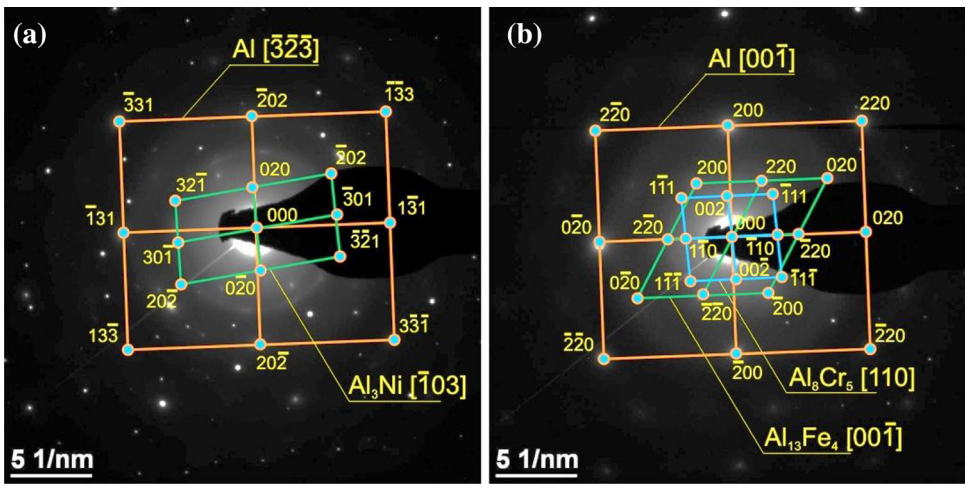

Fig. 5 Diffraction patterns from the alloying zone, **a** Al and Al_3Ni, **b** Al, Al_8Cr_5 and $Al_{13}Fe_4$ phases

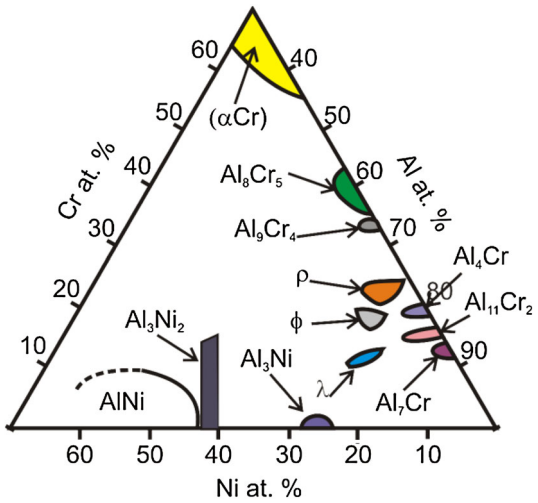

Fig. 6 Ternary phase diagram Al–Ni–Cr [12]

aluminium alloy surface (Table 5). The average wear volume of the laser-alloyed composite layer was more than six times smaller than the wear volume of non-alloyed $AlMg_5Si_2Mn$. The wear track topography and cross-sectional profile of the wear track are shown in Figs. 8 and 9.

During ball-on-disk wear test, friction coefficient between tested sample and ceramic counter-specimen was also registered (Fig. 10). Analysis of friction coefficient results shows that laser-alloyed composite layer of aluminium alloy has a lower friction coefficient when compared to the substrate metal. The average friction coefficient, after distance of 60, was 0.45 in the case of the laser-alloyed composite layer, while for non-alloyed aluminium substrate its value varied over a wear test in the range from 0.49 to 0.69. The average friction coefficient of aluminium alloy substrate during wear test, after reaching 60 m, was equal to 0.44. The changes in the friction

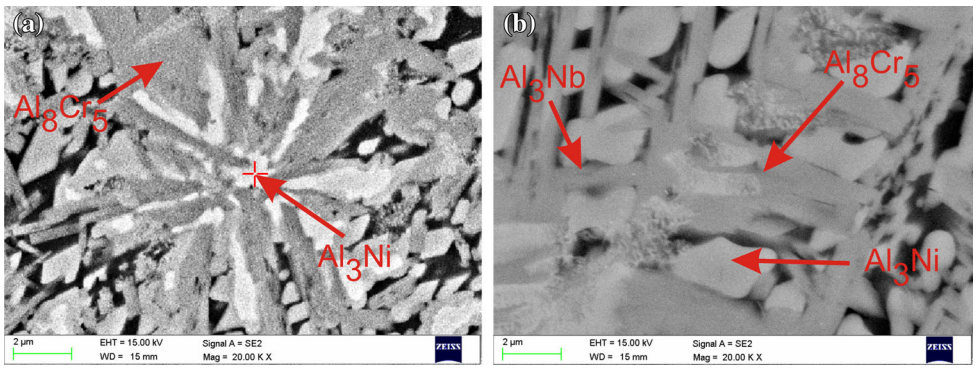

Fig. 7 Microstructure of laser-alloyed aluminium with Inconel 625 powder **a** the central zone of alloying zone; **b** alloying zone about 50 μm from the weld bead

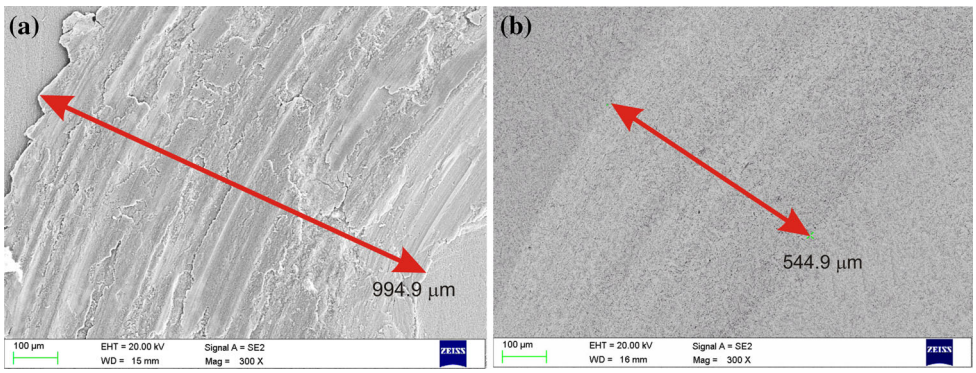

Fig. 8 Ball-on-disk test wear track topography (on the figures wear track width is plotted): **a** non-alloyed $AlMg_5Si_2Mn$ alloy and **b** laser-alloyed composite layer on aluminium alloy

Table 5 Roughness and dimension of the wear track after ball-on-disk test

Material	Roughness of the surface Ra (μm)	Dimension of the wear profile		
		Depth (μm)	Width (mm)	Volume (mm^3)
$AlMg_5Si_2Mn$	1.32	74.8	1.39	0.75
$AlMg_5Si_2Mn$ + Inconel 625	0.21	16.5	0.63	0.12

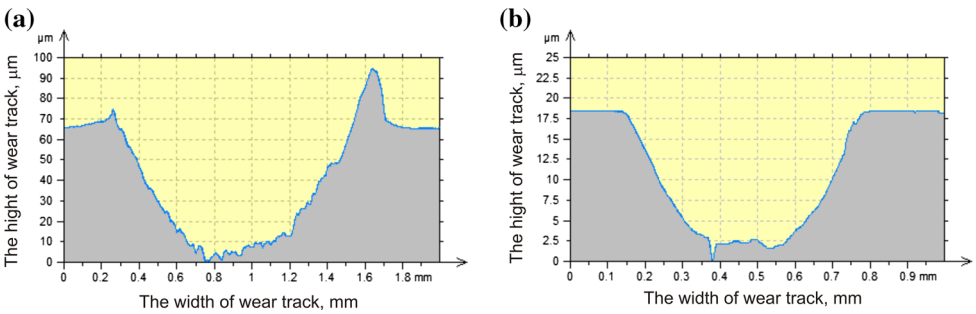

Fig. 9 Ball-on-disk test wear track profile **a** non-alloyed $AlMg_5Si_2Mn$ alloy and **b** laser-alloyed composite layer on aluminium alloy

coefficient of non-alloyed aluminium alloy $AlMg_5Si_2Mn$ are caused by formation of surface material build-up on the counter-specimen surface and its cyclical detachment and pulling the portions of the substrate material (Fig. 8a). In the case of laser-alloyed composite layer on aluminium alloy, it was revealed large changes in friction coefficient in the first stage of the wear test (wear distance up to 50 m). The chemical analysis of wear debris and wear surface topography analysis of the sample after a wear distance of 15 m shows abrupt changes in the friction coefficient in the first stage of wear test. The changes in friction coefficient are caused by the detachment of non-dissolved particles of Inconel powder from the alloyed surface. The presence of undissolved powder particles in

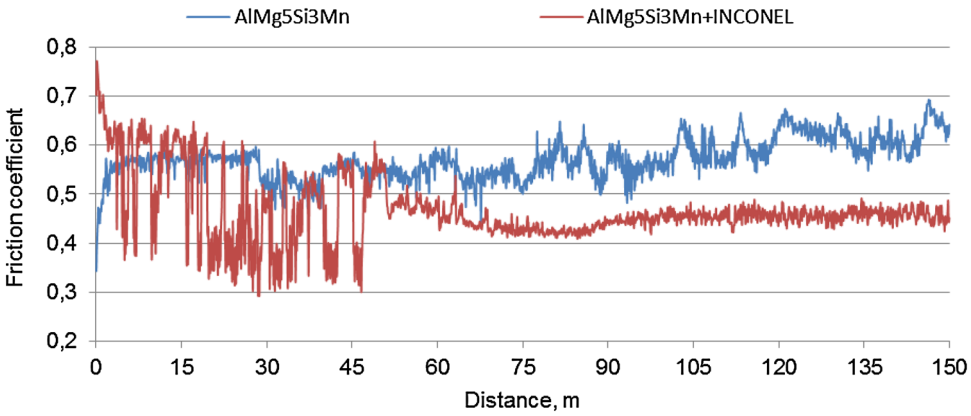

Fig. 10 Friction coefficient during ball-on-disk wear test

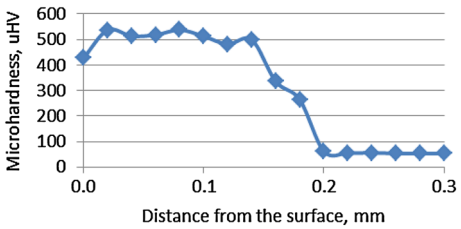

Fig. 11 Microhardness distribution along the cross section of alloyed layer

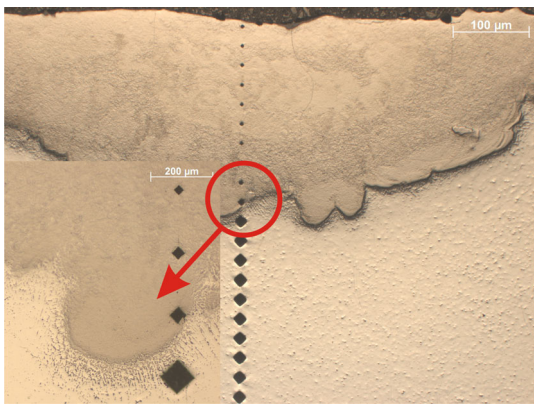

Fig. 12 Vickers microhardness imprints along the cross section of alloyed layer

the wear track during the tribological test causes a sudden change in the friction coefficient. The friction coefficient after a wear distance of 50 m is stabilizing. Undissolved powder particles during wear test are finally removed from contact area due to centrifugal force and do not disturb the process of friction.

It has been proved that the mechanical properties of the alloyed layers, including inter alia, the hardness, depend largely on the resulting microstructure and the quantity and distribution of formed intermetallic phases. The hardness measurements demonstrated a significant increase in the hardness of the laser-alloyed composite layer with regard to the hardness of the substrate alloy $AlMg_5Si_2Mn$. Application of Inconel 625 powder to create the laser-alloyed composite layer increased hardness from 39 to 82 HRA.

The average microhardness of investigated $AlMg_5Si_2Mn$ alloy is about 55 $HV_{0.3}$, while the microhardness measurements made on cross section of the laser-alloyed composite layer shows an increase of about 476 $HV_{0.3}$ (Figs. 11, 12). Performed studies revealed that the hardness of the laser-alloyed composite surface layer is strongly dependent on the microstructure including morphology, hardness and distribution of precipitates formed during alloying (Al_3Ni, Al_3Ni_2, Al_8Cr_5, Al_3Nb and ρ) and ranged from 481 $HV_{0.3}$ at the bottom area to 537 $HV_{0.3}$ in the central part of alloyed zone. The hardness of the crystallizing phase was included in the range from 140 HV for Al_3Ni phase to 780 HV for the Al_3Ni_2 phase. Despite identification of hard and brittle intermetallic phases, such as Al_3Ni, Al_3Ni_2, Al_8Cr_5 in alloyed zone, the disclosed cracks and voids were not observed after hardness test around the penetrator imprint, because the crack propagation of hard precipitates was inhibited by a soft and plastic aluminium matrix (Fig. 11) [26]. In the vicinity of the lower part of alloyed layer, less rich in intermetallic phases, the hardness suddenly begins to decline and stabilize in the area of pure aluminium substrate. The results of microhardness measurement along the cross section of the laser-alloyed composite surface layer are shown in Fig. 11.

4 Conclusions

The study of the microstructure using light and scanning electron microscopy confirmed the presence of the alloyed zone, the transition zone and the heat-affected zone (HAZ) resulting from the laser surface alloying of aluminium alloy EN AC-$AlMg_5Si_2Mn$ with spheroidal Inconel 625 powder

using the fibre laser of wavelength $\lambda = 1070$ nm. The laser-alloyed composite layer shows a plurality of aluminium intermetallic phases rich in chromium and nickel (Al_3Ni, Al_3Ni_2, Al_8Cr_5), and also a few precipitates composed of aluminium and niobium-Al_3Nb as well as ternary phase of chemical composition $Al_{75}Cr_{22}Ni_4$. Furthermore, the analysis of thin films in the transmission electron microscope revealed the presence of precipitates consisting of nickel, iron, chromium, manganese, molybdenum and niobium. Based on tribological studies, a significant increase in wear resistance of the laser-treated surface was evidenced. The wear depth of laser-alloyed composite layer was about 4.5 times smaller than that of the surface of non-alloyed aluminium alloy. The average wear volume of the laser-alloyed surface was more than six times smaller than that of non-alloyed $AlMg_5Si_2Mn$ aluminium alloy. The application of a nickel superalloy powder in the laser alloying process to obtain a composite surface layer has increased the hardness from 39 to 82 HRA. The average superficial microhardness of studied aluminium alloy $AlMg_5Si_2Mn$ was about 55 $HV_{0.3}$, while after laser surface alloying with Inconel powder it was increased about 476 $HV_{0.3}$. Microhardness measurements conducted on the cross section of the surface layer showed a significant increase in the microhardness in the surface layer, compared to the microhardness of the substrate.

As evidenced by presented results, application of the laser surface treatment using high-power fibre laser allows significant improvement in the mechanical properties and wear resistance of studied aluminium alloy, thus contributing to enhance its attractiveness in many fields of possible applications.

Acknowledgments This publication was financed within the framework of the statutory financial grant supported by the Faculty of Mechanical Engineering of the Silesian University of Technology in 2015.

References

1. T. Tański, A.D. Dobrzańska-Danikiewicz, K. Labisz, W. Matysiak, Long-term development perspectives of selected groups of engineering materials used in the automotive industry. Arch. Metall. Mater. **59**(4), 1717–1728 (2014)
2. A.D. Dobrzańska-Danikiewicz, T. Tański, J. Domagała-Dubiel, Unique properties, development perspectives and expected applications of laser treated casting magnesium alloys. Arch. Civil. Mech. Eng. **12**, 318–326 (2012)
3. K. Labisz, Microstructure and mechanical properties of high power diode laser (HPDL) treated cast aluminium alloys. Materialwiss. Werkstofftech. **45**(4), 314–324 (2014)
4. T. Tański, Determining of laser surface treatment parameters used for light metal alloying with ceramic powders. Mater. Sci. Eng. Technol. **45**(5), 333–343 (2014)
5. T. Tański, P. Snopiński, W. Pakieła, W. Borek, S. Rusz, Structure and properties of AlMg alloys after combination of ECAP and post-ECAP aging. Arch. Civil Mech. Eng. **16**(3), 325–334 (2016). doi:10.1016/j.acme.2015.12.004
6. J. Konieczny, K. Labisz, J. Wieczorek, L.A. Dobrzański, Stereometry specification of anodised and PVD coated surface of aluminium alloy. Arch. Mater. Sci. **38**(2), 85–92 (2009)
7. J. Kusiński, S. Kac, A. Kopia, A. Radziszewska, M. Rozmus-Górnikowska, B. Major, L. Major, J. Marczak, A. Lisiecki, Laser modification of the materials surface layer—a review paper. Bull. Pol. Acad. Sci. **60**, 711–728 (2012)
8. A. Lisiecki, Welding of thermomechanically rolled fine-grain steel by different types of lasers. Arch. Metall. Mater. **59**(4), 1625–1631 (2014). doi:10.2478/amm-2014-0276
9. A. Lisiecki, in Welding of titanium alloy by Disk laser. Proceedings of SPIE, Laser Technology, Applications of Lasers (2013), p. 87030
10. D. Janicki, Improvement of wear resistance of stainless steel AISI 304L by diode laser surface alloying with chromium carbide. Appl. Mech. Mater. **809–810**, 363–368 (2015). doi:10.4028/www.scientific.net/AMM.809-810.363
11. T. Tański, W. Pakieła, D. Janicki, B. Tomiczek, M. Król, Properties of the aluminium alloy EN AC-51100 after laser surface treatment, Arch. Met. Mater. **61**(1), 199–204 (2016). doi:10.1515/amm-2016-0034
12. D.N. Compton, L.A. Cornish, M.J. Witcomb, The effect of microstructure on hardness measurements in the aluminium-rich corner of the Al–Ni–Cr system. J. Alloy. Compd. **317–318**, 372–378 (2001)
13. A. Almeida, P. Petrov, I. Nogueira, R. Vilar, Structure and properties of Al–Nb alloys produced by laser surface alloying. Mater. Sci. Eng. A **303**, 273–280 (2001)
14. B. Grushkoa, W. Kowalski, D. Pavlyuchkova, S. Mi, M. Surowieca, Al-rich region of the Al–Ni–Cr alloy system below 900 °C. J. Alloy. Compd. **485**(1–2), 132–138 (2009)
15. H.-F. Xuana, Q.-Y. Wanga, S.-L. Baia, Z.-D. Liub, H.-G. Sunc, P.-C. Yanc, A study on microstructure and flame erosion mechanism of a graded Ni–Cr–B–Si coating prepared by laser cladding. Surf. Coat. Technol. **244**, 203–209 (2014)
16. Patent Number: PL405550-A1, Publ. Date 13 Apr 2015, Method for laser alloying of aluminum substrate and ceramic particles of aluminum alloys, involves providing substrate with laser alloying of aluminum and aluminum alloys ceramic particles, and feeding powder from liquid weld pool, Inventor(s): Janicki D, Tanski T, Labisz K, Pakiela W, Lisiecki A, Patent Assignee: Politechnika Slaska Pstrowski, Derwent Primary Accession Number: 2015-30743R
17. A. Lisiecki, Titanium matrix composite Ti/TiN produced by diode laser gas nitriding. Metals **5**(1), 54–69 (2015). doi:10.3390/met5010054
18. J. Kusiński, S. Kac, A. Kopia, A. Radziszewska, M. Rozmus-Górnikowska, B. Major, L. Major, J. Marczak, A. Lisiecki, Laser modification of the materials surface layer—a review paper. Bull. Pol. Acad. Sci. Techn. Sci. **60**(4), 711–728 (2012)
19. D. Janicki, High power diode laser cladding of wear resistant metal matrix composite coatings. Solid State Phenom. Mechatron. Syst. Mater. **199**, 587–592 (2013). doi:10.4028/www.scientific.net/SSP.199.587
20. Patent Number: PL403146-A1, Publ. Date15 Sep 2014, Integrated system for protection of area during liquid and/or powder metal feeding process for single-substrate laser alloying of magnesium and magnesium alloys, has protective gas nozzle and powder feed nozzle arranged to each other. Inventor(s): D. Janicki, T. Tanski, K. Labisz, A. Lisiecki, Patent Assignee: Politechnika Slaska Pstrowski, Derwent Primary Accession Number: 2015-21527S

21. L.A. Dobrzański, T. Tański, A.D. Dobrzańska-Danikiewicz, E. Jonda, M. Bonek, A. Drygała, in Structures, properties and development trends of laser-surface-treated hot-work steels, light metal alloys and polycrystalline silicon, ed. by J. Lawrence, D. Waugh (eds.), Laser Surface Engineering. Processes and Applications, (Woodhead Publishing Ltd., UK, 2015), pp. 3–32 (ISBN 978-1782420743)
22. A. Almeida, M. Anjos, R. Vilar, R. Li, M.G.S. Ferreira, Laser alloying of aluminium alloys with chromium. Surf. Coat. Technol. **70**, 221–229 (1995)
23. Y. Fu, A.W. Batchelor, Y. Gu, K.A. Khor, H. Xing, Laser alloying of aluminum alloy AA 6061 with Ni and Cr. Part 1. Optimization of processing parameters by X-ray imaging. Surf. Coat. Technol. **99**(3), 287–294 (1998)
24. A. Almeidaa, P. Petrovb, I. Nogueiraa, R. Vilara, Structure and properties of Al–Nb alloys produced by laser surface alloying. Mater. Sci. Eng. A **303**(1-2), 273–280 (2001)
25. R. Vilara, O. Condeb, S. Francoa, Crystallographic structure of Al_3Nb in laser-processed Al–Nb alloys. Intermetallics **7**(11), 1227–1233 (1999)
26. C.T. Rios, A.A. Coelho, W.W. Batista, M.C. Gonçalves, R. Caram, ISE and fracture toughness evaluation by Vickers hardness testing of an Al_3Nb–Nb_2Al–AlNbNi in situ composite. J. Alloys Compd. **472**(1–2), 65–70 (2009)